NUMERICAL STUDY ON OXY-BIOMASS CO-FIRING IN A CEMENT ROTARY KILN

by

Yixiang SHU[a], Hanlin ZHANG[a], Jiaye ZHANG[a], Wei XU[b], Yanlong CHENG[c], Su ZHANG[a], Hrvoje MIKULČIĆ[d], Yuhan LIAO[e], Zhaochen SHI[a], Yang GUO[a], and Xuebin WANG[a*]

[a]MOE Key Laboratory of Thermo-Fluid Science and Engineering, Xi'an Jiaotong University, Xi'an, China
[b]Jidong Heidelberg (Jingyang) Cement Co., Ltd., China
[c]Shanghai Institute of Special Equipment Inspection and Technical, Changhai, China
[d]Faculty of Mechanical Engineering and Naval Architecture, University of Zagreb, Zagreb, Croatia
[d]City University of Hong Kong, Hong Kong, China

Original scientific paper
https://doi.org/10.2298/TSCI2405407S

Cement manufacturing is among the industries with the highest energy consumption and pollution emissions. Combining oxy-fuel combustion with the technology of co-firing biomass with coal is a promising way to reduce pollutant and carbon emissions. Based on a 6000 t per day cement rotary kiln, the performance of oxy-biomass co-firing technology is investigated by CFD modeling. Cases under different biomass ratios (0%-30%) and O_2 concentrations are simulated. Combustion characteristics including temperature field, wall heat flux distribution, NO_x emissions, etc. are widely assessed. It is found that biomass co-firing can significantly reduce ignition delay caused by high CO_2 concentration during oxy-fuel combustion. A flame distribution similar to the conventional air-fired condition is obtained under conditions of 33% O_2 concentration and 10% biomass co-firing ratio. The wall heat transfer is enhanced in oxy-fuel cases. With the increase of biomass co-firing ratio, the wall heat flux tends to be more uniform. Oxy-fuel combustion can effectively reduce NO_x emissions and the fuel-N conversion ratio. Biomass co-firing under oxy-fuel conditions can reduce the fuel-N conversion ratio from 10.9% to 8%, but it will lead to a slight increase in NO_x emissions from 848 ppm to 899 ppm. It is necessary to control the co-firing amount of biomass to achieve effective combustion and pollutant emission control.

Key words: *cement rotary kiln, numerical simulation, oxy-fuel combustion, biomass co-firing, NO_x emissions*

Introduction

Cement production is a typical high-energy consumption and high-pollution industry. It was calculated that the emissions from this process contributed around 5% of anthropogenic CO_2 emissions [1]. Unlike other processes, the process chemistry plays a more important role in CO_2 emissions than fossil fuel combustion. About 60% of CO_2 emissions come from the calcination process of raw meals. As a whole, the production of one kilogram of cement releases about 0.6-0.7 kg of CO_2 [2]. To delay global warming and realize the 1.5 ℃

* Corresponding author e-mail: wxb005@mail.xjtu.edu.cn

temperature rise target of the Intergovernmental Panel on Climate Change, carbon capture technology must be adopted in the cement industry to achieve carbon reduction [3].

Oxy-fuel combustion is a promising carbon capture technology for massive carbon capture [4]. It has been identified as a carbon capture technology that could achieve a high capture efficiency at a lower cost [5]. The air works as an oxidant in traditional combustion, and the N_2 in the air reduces the amount of CO_2 in the exhaust gas. The extraction of CO_2 from these thin mixtures is a costly and intricate process. Oxy-fuel combustion is the term for the combustion process in which ordinary air is replaced by either pure O_2 or a combination of CO_2 and O_2. The primary component of the flue gas is CO_2 and H_2O due to the removal of N_2 from the combustion medium. A condensation procedure of the exhaust gas is used to extract H_2O and create nearly pure CO_2. After that, the pure CO_2 can be extracted and used for sequestration, increased oil recovery, or the injection of CO_2 into depleted oil and gas reservoirs [6, 7]. The carbon capture ratio is predicted to be more than 90% [8]. The application of oxy-fuel combustion technology in power plants has been widely discussed [9-13]. However, little experience can be transferred to cement production because of distinctions in boundary conditions and configuration.

At present, the oxy-fuel combustion technology applied in cement production mainly focuses on calciner and rotary kilns. By using an oxy-fuel combustion configuration in the calciner, more than 60% of CO_2 emissions can be captured, making it a very promising carbon capture method [2]. However, modifications are needed to address the issue of air leakage in the preheating tower. Meanwhile, oxy-fuel combustion may cause changes in the clinker. A reasonable configuration is needed to avoid this impact. The application in rotary kilns requires adjusting the burner to adapt to the implementation of oxy-fuel combustion. The existing oxy-fuel combustion application of the cement process is only aimed at calciner. The FLSmidth R&D 2-3 tph pilot plant located in Dania, Denmark has successfully conducted the first pilot plant tests of the calciner oxy-fuel combustion [14]. Application about oxy-fuel combustion in cement rotary kilns still remains on laboratory scale.

In the cement production process, energy costs account for 50% to 60% of total production costs, while fuel costs are equivalent to 20% to 25% of total production costs. About 40% of the thermal energy is used for the combustion of rotary kiln, and about 60% of the thermal energy is used for the calcination process in the calciner [2]. To reduce environmental pollution and fuel costs, many cement producers choose to use alternative fuels, such as municipal waste and industrial waste. This has already achieved good development in the past few decades. Biomass is also considered a potential alternative energy source for cement production [15]. Because of the difference in the oxidizer and the atmosphere in kilns, oxy-fuel combustion affects the combustion process of fuel as well as the related processes such as heat transfer. It was reported that high CO_2 levels can impact negatively on fuel ignition and temperature distribution. Pilot-scale testing revealed that supplying enough O_2 to the pulverized coal flame is crucial for ensuring a decent ignition and flame stability in oxy-fuel systems [16]. Biomass is a carbon neutral fuel that expected to be the most promising alternative energy source to fossil fuel, and biomass co-firing could bring benefits to oxy-fuel combustion [17-20]. Compared with fuel coal, biomass has a higher volatile content, which makes it easier to ignite. By co-firing biomass instead of increasing O_2 concentration, the ignition performance of fuel can be improved, and the ignition and temperature distribution of cement kiln oxy-fuel combustion may also be improved. Wang *et al.* [21] reported that the addition of biomass helps to improve temperature uniformity. In addition, biomass can substitute for part of coal fuel to save fuel costs and further reduce carbon emissions. Biomass co-firing has the po-

tential for improving oxy-fuel combustion in rotary kiln. However, there is still little research on oxy-biomass co-firing in cement kilns. By biomass co-firing, it is possible to reduce the adverse effects of oxy-fuel combustion on cement production process. It is expected to achieve flame and emission control without changing the existing cement kiln structure, and improve the application of oxy-fuel combustion on traditional cement kilns in a very economical and environmentally friendly way.

In this paper, the influence of oxy-biomass co-firing is investigated based on a 6000 t per day cement rotary kiln. Cases under different biomass ratio (0%-30%) and O_2 concentrations are simulated. Combustion characteristics including temperature field, wall heat flux distribution, NO_x emissions, *etc*. are studied. This study aims at improving the understanding of the oxy-biomass co-firing process and optimize the combustion process inside the rotary kiln for further carbon emissions reduction.

Materials and methods

Fuel properties

The coal and biomass involved in this paper are Guasare coal and olive waste, and their properties are listed in tab. 1. Considering that the mean particle size of biomass particles is only 100 mm, isothermal assumption and Rosin-Rammler diameter distribution is adopted.

Table 1. Proximate and ultimate analysis of fuels

Name	Proximate analysis [wt.%]				Ultimate analysis [wt.%]				
	M_{ar}	A_{ar}	V_{ar}	FC_{ar}	C_{daf}	H_{daf}	N_{daf}	O_{daf}	S_{daf}
Coal	2.9	3.3	37.1	56.7	81.6	5.5	1.5	10.7	0.6
Biomass	9.0	6.9	65.4	18.7	54.3	6.6	1.95	36.9	0.22

Geometry, mesh, boundary conditions, and calculation cases

This work is based on a 6000 t per day cement rotary kiln and its burner. The model of the rotary kiln and burner is illustrated in fig. 1. The length of the rotary kiln is 72 m, and the inner diameter is 4550 mm. The temperature of primary air, including central flow, coal flow, swirl flow, and axial flow, is 320 K and the secondary air is heated to 1473 K.

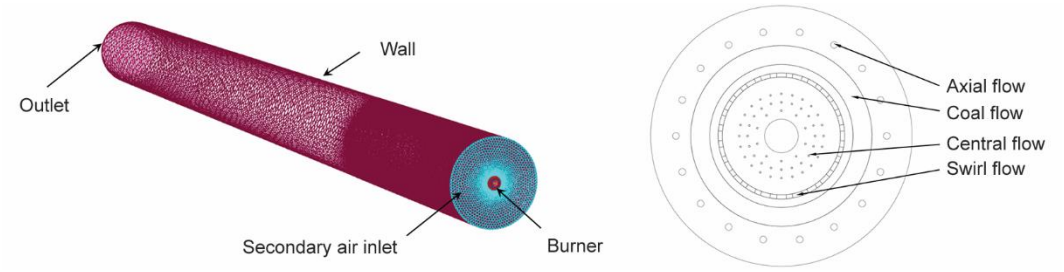

Figure 1. Geometry and mesh of rotary kiln and burner

The poly-hexcore type meshes are generated by FLUENT MESHING. The results of mesh independence validation are shown in fig. 2. The calculation results of the average temperature, T_m, and maximum temperature, T_{max}, at 7 m, and 10 m from the kiln head are com-

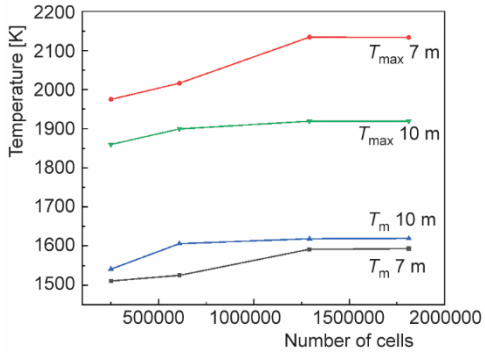

Figure 2. Mesh independence verification

pared for meshes with different cell numbers. There is no significant difference when the number of cells is above 1291473, so the mesh with 1291473 cells is selected for calculation.

The boundary conditions are set to velocity-inlet and pressure-outlet. The burner wall is specified as adiabatic, and the rotary kiln wall is set to 1200 K. The calculation of the biomass co-firing ratio is based on the ratio of biomass combustion heat to total combustion heat. Two cases are calculated under air-fired conditions, four cases are calculated under oxy-coal conditions, and three oxy-fuel cases are calculated under 33% O_2 concentration with a 10%-30% biomass co-firing ratio. On the rotary kiln involved in this paper, stable combustion cannot be realized under oxy-fuel conditions with 21% O_2 concentration.

Numerical model

The CFD modeling of oxy-fuel combustion uses methods and sub-models which are similar to air-fired situations. The present sub-models, which were developed for air-fired combustion, may not be accurate enough in a high CO_2 atmosphere [12]. The model selection of oxy-fuel cases will be discussed below.

Turbulence and radiation model

The realizable k-ε model is used to solve the turbulence equation, which fits rotation and strong recirculation turbulent flow very well [21]. The discrete ordinate approach is used to describe the transport of radiant heat. Lagrangian particle tracking is used to simulate the dispersed particle phase. The P1 model, which is usually used in combustion simulations, is chosen to calculate the radiation transfer [22]. The high concentration of CO_2 under the oxy-fuel mode will lead to a different radiation pattern. Yin *et al.* [23] reported a new weighted sum of gray gases model that fits large-scale oxy-fuel simulation well. This model is imported into FLUENT through user defined functions to simulate the oxy-fuel cases of cement rotary kilns.

The volatile of coal is replaced by pseudo-species. The EDC model is used to model turbulent chemistry interaction. Two-competing rate devolatilization model and multi-surface reaction model, which have been widely validated to be efficient for coal combustion [24], are applied in this work. Meanwhile, a single rate model is adopted for biomass devolatilization [21]. The reaction kinetic parameters of devolatilization and surface reaction model are listed in tabs. 2 and 3, respectively.

Table 2. Parameters of the devolatilization model

Fuel	Pre-exponential factor	Activation energy	Weighting factor
Coal	200000	$1.046 \cdot 10^{08}$	0.3
	$1.3 \cdot 10^{07}$	$1.674 \cdot 10^{08}$	1
Biomass	$4.3106 \cdot 10^{07}$	$8.3492 \cdot 10^{07}$	–

Table 3. Reaction mechanism

Reaction	Rate exponent	A [s^{-1}]	E [$Jkmol^{-1}$]	b
$C_xH_yO_z + \frac{x-z}{2}O_2 = xCO + \frac{y}{2}H_2$	$[C_xH_yO_z][O_2]$	$3.8 \cdot 10^{07}$	5.55×10^7	0
$CO + H_2O = CO_2 + H_2$	$[CO][H_2O]$	$2.75 \cdot 10^{09}$	8.37×10^7	0
$CO_2 + H_2 = CO + H_2O$	$[CO_2][H_2]$	$6.81 \cdot 10^{08}$	1.14×10^8	0
$H_2 + 0.5O_2 = H_2O$	$[H_2]^{0.25}[O_2]^{1.5}$	$6.8 \cdot 10^{15}$	1.67×10^8	–1
$C + H_2O = CO + H_2$	$[H_2O]$	0.00192	1.47×10^8	0
$C + 0.5O_2 = CO$	$[O_2]$	0.005	7.4×10^7	0

The NO_x model

The NO_x formation is performed using a post-processing technique, based on the concentrations, velocity, and temperature fields calculated beforehand [25]. The NO_x generated during solid fuel combustion is mainly through three pathways, including thermal NO_x, fuel NO_x, and prompt NO_x. The expressions for the rate coefficients for these reactions refer to Hanson's work. [26].

According to the De Soete mechanism [27], fuel NO_x is often thought to occur by the creation of HCN and/or NH_3, which are oxidized to NO while being competitively reduced to N_2. The prompt NO_x is not taken into consideration in this study since it is paltry compared to the others.

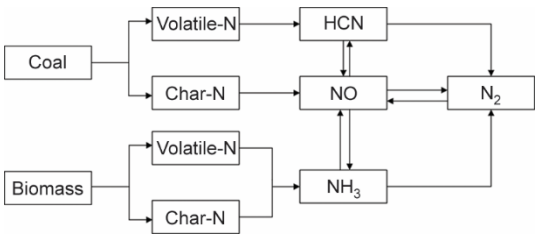

Figure 3. Transformation pathway of N_2

The pathways of NO_x formation of coal and biomass combustion are illustrated in fig. 3. In many previous studies, the nitrogen in coal transfers to HCN and NO [28-30], while the nitrogen in olive waste transforms into ammonia [31-33].

The NO_x reduction by char is demonstrated by:

$$\frac{dNO}{dt} = 230e^{-\frac{142737}{RT}} A_E P_{NO} \tag{4}$$

where A_E is the surface area of the char and P_{NO} – the partial pressure of the NO.

A partial equilibrium method is used to calculate the NO_x reduction by the hydrocarbons, and the equivalent reduction fuel in this work is CH_4.

Results and discussion

Model validation

Because of the rotation, it is challenging to measure the inside temperature of the kiln. The experimental validation is based on outlet flue gas parameters. The comparison between the experimental and simulated values at the outlet under air-fired conditions is shown

in tab. 4. The simulation results align well with the experimental data, hence further studies about oxy-biomass co-firing in the rotary kiln will be based on this simulation model.

Table 4. Validation of temperature, O_2 and NO concentration at outlet

Name	Measurement value	Simulation value
Outlet temperature	1041 °C	1013
Flue gas O_2	2.25 mol.%	2.84%
Flue gas NO_x	1826	1806

Simulation results of oxy-biomass co-firing

Temperature predictions

The temperature fields of air-fired and oxy-fuel combustion cases are illustrated in fig. 4. In fig. 4(b), air/oxy correspond to air-fired/oxy-fuel conditions, respectively. Oxy24 means an oxy-fuel condition with 24% O_2 concentration. The percentage corresponds to the biomass co-firing proportion. Compared to air-fired conditions, the maximum combustion temperature under oxy-fuel conditions is lower, and its temperature field is more moderate. The ignition delay increases significantly under high CO_2 levels, resulting in the high temperature zone of the flame moving backward. The reason for the phenomenon is that the specific heat of CO_2 is significantly higher than that of N_2, and high concentrations of CO_2 have a negative effect on the ignition of coal particle [16]. In addition, the flame speed of pulverized-coal cloud under oxy-fuel conditions is slower than that in air-fired conditions [34]. As the O_2 concentration increases, the maximum combustion temperature gradually increases, while the ignition delay decreases. A similar highest combustion temperature to air-fired condition was achieved at 33% O_2 concentration, which is consistent with the report of Molina and Shaddix [35].

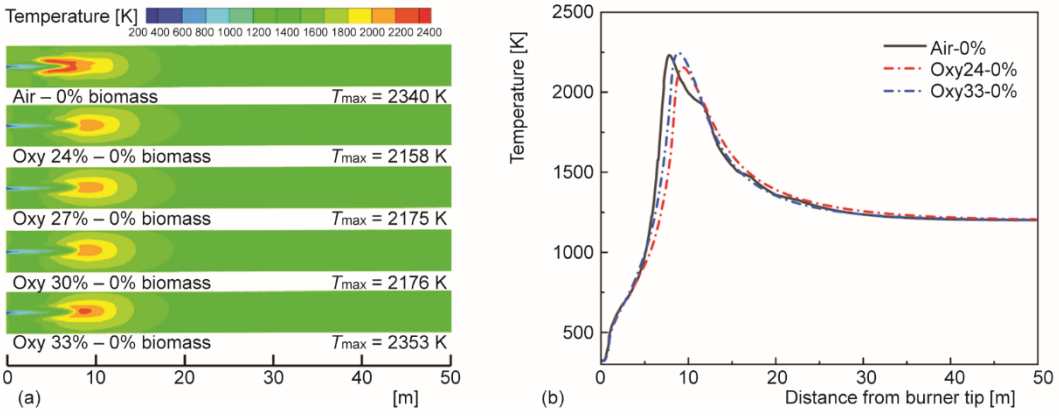

Figure 4. Comparison of temperature fields between air-fired and oxy-fuel conditions; (a) temperature contours and (b) temperature distribution along the central axis

The temperature fields of coal-fired and biomass co-firing cases are illustrated in fig. 5. Biomass co-firing results in a significant forward movement of flame and a reduction in

ignition delay both in air-fired mode and oxy-fuel mode. For air-fired cases, the temperature gradient decreases after biomass co-firing, but the maximum temperature slightly increases, reaching 2385 K. On the contrary, the maximum temperature decreases with increasing co-firing ratio for oxy-fuel combustion. This phenomenon agrees with report by Wang *et al.* [21]. This is because biomass has more volatile components and ignites faster. Meanwhile, N_2 has a lower specific heat than CO_2, resulting in an increase in the maximum combustion temperature. Under oxy-fuel conditions, due to the high moisture content in biomass combustion flue gas, the specific heat of the flue gas further increases, highlighting the impact of the low calorific capacity of biomass.

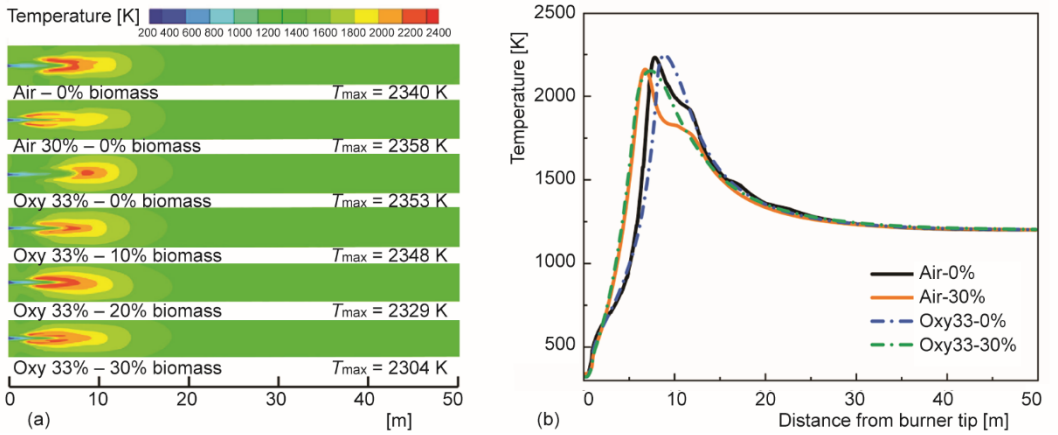

Figure 5. Comparison of temperature fields between coal-fired and biomass co-firing conditions; (a) temperature contours and (b) temperature distribution along the central axis

To further quantify and analyze the macroscopic characteristics of combustion in rotary kilns, the volumetric average temperature, T_v, and temperature field non-uniformity coefficient, C_w, are defined:

$$\bar{T}_v = \frac{\int_v T_v \mathrm{d}v}{V} \tag{5}$$

$$C_w = \sqrt{\frac{1}{V}\frac{\int_v (T_v - \bar{T}_v)^2 \mathrm{d}v}{\bar{T}_v^2}} \tag{6}$$

where T_v is the temperature of micro volumes in the rotary kiln and V – the volume of the rotary kiln hearth.

According to fig. 6, oxy-fuel combustion has a higher T_v but a more uniform temperature field compared to air-fired combustion. As the O_2 concentration increases, the volumetric average temperature decreases, but the kiln temperature field becomes more non-uniform. After biomass co-firing, T_v and C_w under air combustion conditions have significantly decreased. This indicates that biomass co-firing makes the combustion process milder and more uniform in air-fired mode. However, biomass co-firing leads to an increase in the volumetric average temperature and temperature non-uniformity of the rotary kiln in oxy-fuel mode.

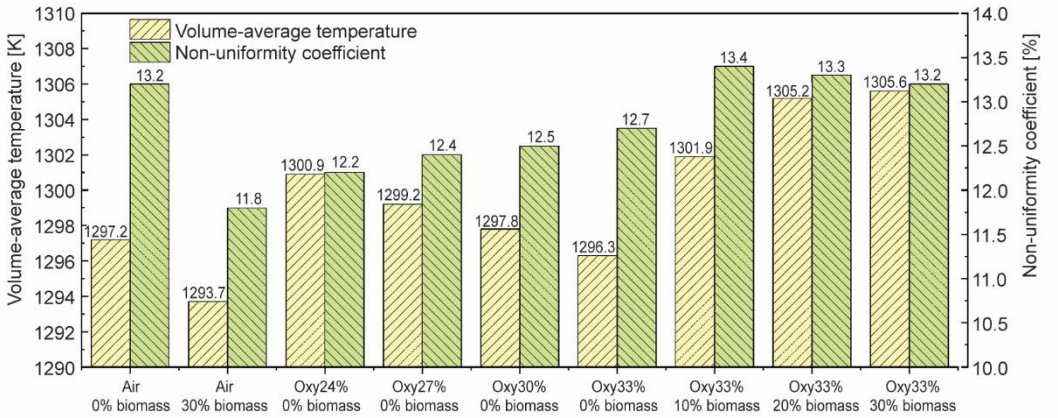

Figure 6. Volumetric average temperature and temperature field non-uniformity coefficient in different cases

Heat transfer

Figure 7 shows the distribution of heat flux on the bottom wall of the rotary kiln. Under coal-fired conditions, the high heat flux area of oxy-fuel condition moves significantly backward, and the wall heat flux is more concentrated. This is mainly due to the ignition delay and the strong radiation ability of CO_2. The heat transfer in cement kilns mainly depends on radiation. The content of CO_2 and H_2O in the flue gas of oxy-fuel combustion is very high, which is not transparent to radiation compared to N_2. This characteristic leads to a great influence on radiation behavior [2]. Study by Andersson *et al.* [36] suggests that gas radiation intensity increases greatly due to the high proportion of CO_2. The wall heat flux distribution after biomass co-firing significantly becomes uniform under both air-fired and oxy-fuel modes. Due to the movement of the flame, the high heat flux area also moves towards the kiln head, and greatly improves the uniformity of heat flow distribution, making the heat flux distribution under oxy-fuel combustion conditions close to the initial air combustion conditions. This indicates that the co-firing oxy-biomass co-firing has great potential for the modification of existing cement kilns.

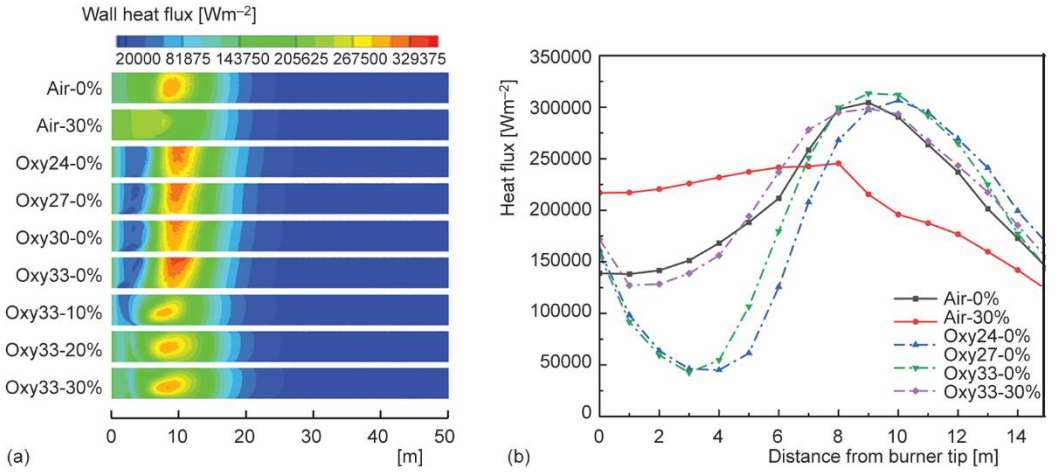

Figure 7. Heat flux on the bottom wall of rotary kiln

The radiation ratio, radiative and convective heat transfer on the wall in different cases are listed in fig. 8. The radiation heat transfer and convective heat transfer on the kiln wall increase under oxy-fuel conditions. The change in biomass co-firing rate has no significant impact on the proportion of radiative heat transfer.

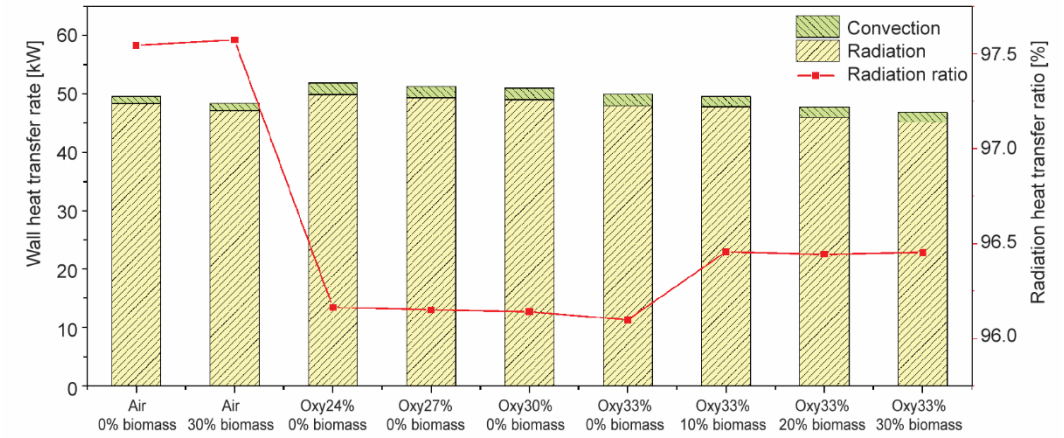

Figure 8. Composition and proportion of wall heat transfer

Species

The concentrations of O_2 along the central axis of the kiln are presented in fig. 9. The O_2 distribution inside the rotary kiln can be divided into three parts. As shown in fig. 9(a), the O_2 concentrations on the centerline of the kiln in different cases begin to decrease at 3 m to 5 m, while the primary flow has been ignited at 2 m to 5 m according to fig. 4. This creates a strong oxidation zone. At 7 m to 10 m, O_2 concentration sharply goes down, while the secondary air is not fully mixed, creating a strong reducing zone. There is a complete lack of O_2 area 8 m away from the burner tip in air-fired cases. In areas above 10 m, the secondary air gradually mixes with the primary air, resulting in an increase in O_2 content.

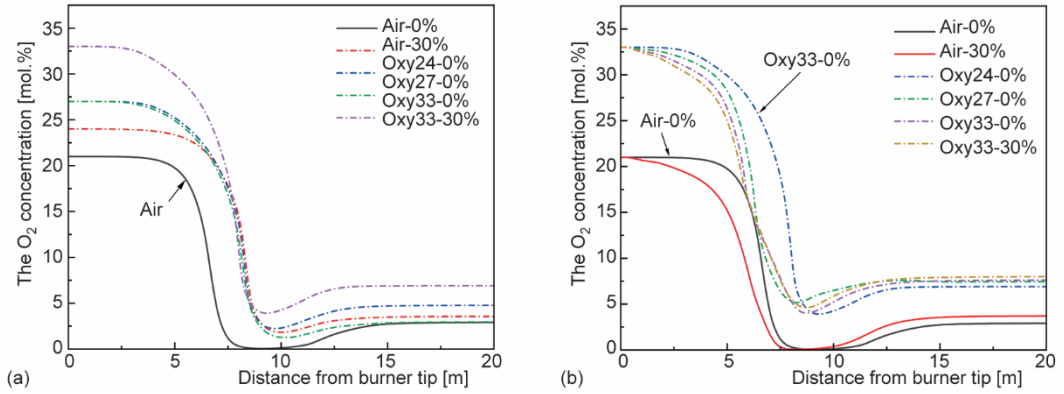

Figure 9. The O_2 distribution along the central axis; (a) air-fired/oxy-fuel condition and (b) biomass co-firing

The volatile content distributions along the central axis in different cases are illustrated in fig. 10. Compared to air-fired conditions, the release of volatile content is delayed

under oxy-fuel conditions, but the maximum concentration of volatile matter increases. After biomass co-firing, the release of volatile matter is significantly accelerated, causing the highest volatile content concentration area to de*via*te from the central axis of the kiln, and the maximum concentration of volatile matter at the central axis shows a downward trend with the increase of biomass co-firing ratio.

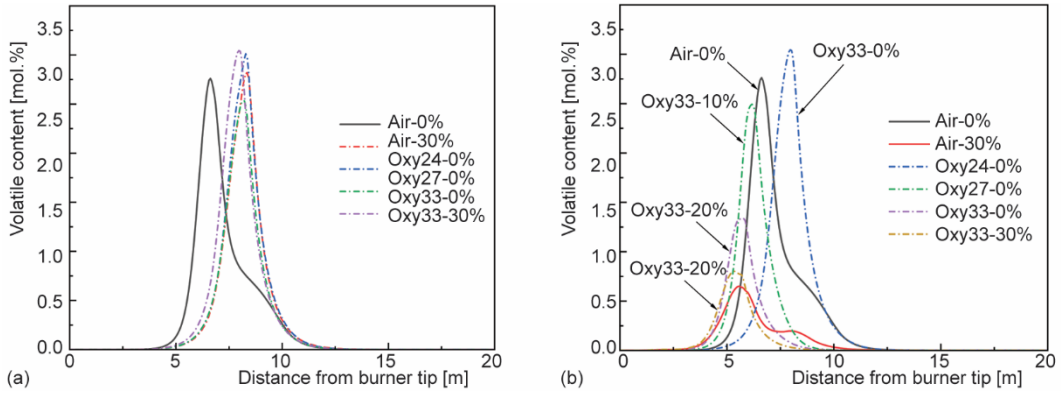

Figure 10. Volatile distribution along the central axis; (a) air-fired/oxy-fuel condition and (b) biomass co-firing

The NO_x distributions along the central axis are shown in fig. 11. Compared with air-fired conditions, the generations of NO_x under oxy-fuel conditions are significantly reduced, and there is a NO_x reduction zone at 8 m to 12 m. In the air-fired case, the generation of NO_x is significantly reduced after biomass co-firing, and the effect of the NO_x reduction zone at 10 to 15 m is enhanced. However, in oxy-fuel cases, the peak value of NO_x generation decreases when co-firing biomass, but the final emissions are not significantly affected.

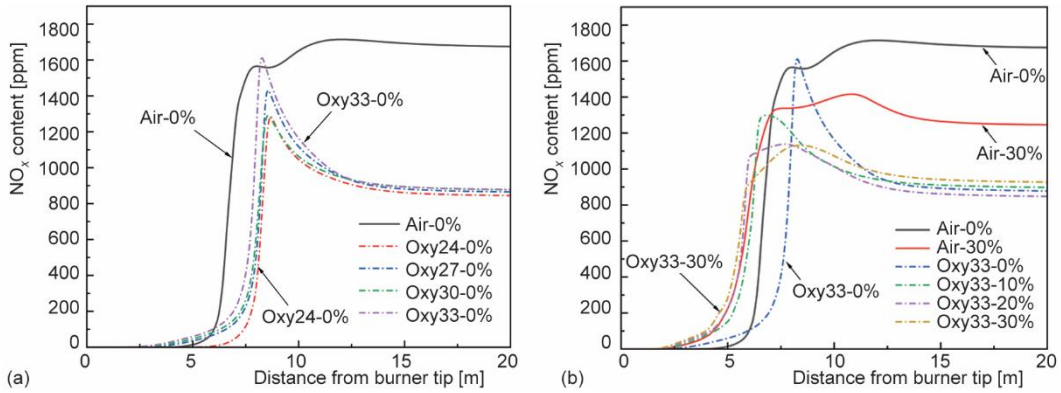

Figure 11. The NO_x distribution along the central axis; (a) air-fired/oxy-fuel condition and (b) biomass co-firing

Considering the changes in the combustion atmosphere and the different N_2 content of the two fuels, the fuel-N conversion fraction of the mixed fuel is defined [21]:

$$\omega_{\mathrm{N}} = \frac{W_{\mathrm{NO}}(m_{\mathrm{oxy}} + m_{\mathrm{coal}} f_1 + m_{\mathrm{bio}} f_2) M_{\mathrm{N}}}{(m_{\mathrm{coal}} f_1 W_{\mathrm{N},1} + m_{\mathrm{bio}} f_2 W_{\mathrm{N},2}) M_{\mathrm{NO}}} \tag{7}$$

where W_{NO} is the NO mass fraction of in flue gas, m_{oxi} – the O_2 mass-flow, m_{coal} and m_{bio} – the mass-flows of coal and biomass, f_1 and f_2 – the burnout rates of coal and biomass, M_N and M_{NO} – the molecular weights of N_2 and NO, and $W_{N,1}$ and $W_{N,2}$ – the N_2 mass fractions in coal and biomass. The NO_x emissions and fuel-N conversion ratios in different cases are plotted in fig. 12.

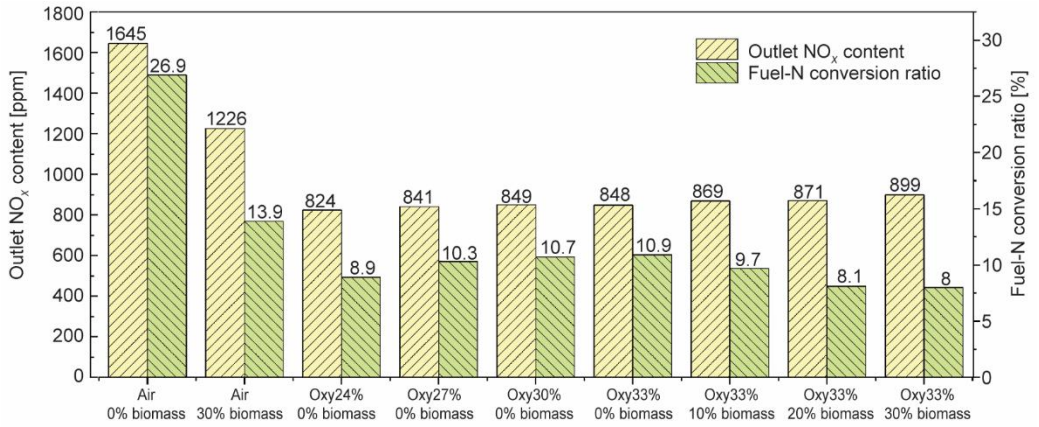

Figure 12. The NO_x emissions at the furnace outlet

As shown in fig. 12, NO_x emissions and fuel-N conversion ratios are significantly reduced under oxy-fuel conditions. This is due to the exclusion of N_2 from combustion, which has a direct impact on the formation of thermal NO_x. The high CO_2 concentration atmosphere and biomass co-firing result in a higher concentration of volatile content field. The effect of O_2 concentration on NO_x emissions and fuel-N conversion ratios in oxy-fuel conditions is not significant, and both of them slightly increase with the increase of O_2 concentration. Under air-fired conditions, biomass co-firing significantly reduces NO_x emissions and fuel-N conversion ratios, which is due to the larger reduction zone caused by biomass pyrolysis and combustion. Under oxy-fuel conditions, biomass co-firing resulted in a slight increase in NO_x emissions and a decrease in the fuel-N conversion rate. This is due to the fact that the main source of NO_x emissions in oxy-fuel mode is fuel NO_x, the high N_2 content of biomass leads to an increase in NO_x generation. However, due to the inhibitory effect of biomass co-firing on NO_x generation, some of the increased fuel-N is not converted into NO_x, and the overall fuel-N conversion ratios of the mixed fuel further decrease.

Conclusions

This article investigates the characteristics of the oxy-biomass co-firing process in cement kilns. The authors studied the temperature fields, species, and kiln wall heat flux in a rotary kiln under different combustion atmospheres (air/oxy24%-33%) and biomass co-firing ratios (0%-30%). The main conclusions are as follows.

An oxy-fuel atmosphere can lead to a decrease in the maximum combustion temperature and ignition delay, while biomass co-firing can reduce ignition delay. A flame distribution similar to the initial air-fired condition is obtained under conditions of 33% O_2 concentration and 10% biomass co-firing ratio. Compared to air-fired cases, wall heat transfer is enhanced in oxy-fuel cases. The wall heat flux tends to be more uniform with the increase in bi-

omass ratio, and the wall heat flux distribution is more similar to the initial air-fired case. The radiative heat transfer ratio under oxy-fuel conditions is lower than that under air-fired conditions. Oxy-fuel combustion can effectively reduce NO_x emissions and the fuel-N conversion ratio. Under oxy-fuel conditions, biomass co-firing can reduce the fuel-N conversion ratio from 10.9% to 8%, but it will lead to a slight increase in NO_x emissions from 848 ppm to 899 ppm. It is necessary to control the co-firing amount of biomass. It is worth noting that the boundary conditions in this study were directly set, and the impact of flue gas recirculation in actual situations was not taken into account. In further research, it is necessary to consider the accumulation and reduction effects of NO_x caused by flue gas recirculation.

Acknowledgment

The authors gratefully acknowledge the financial support of the National Key R&D Program of China (No. 2022YFE0206600) and the National Natural Science Foundation of China (No.52376125).

References

[1] Koring, K., *et al.*, Deployment of CCS in the Cement Industry, IEA Technical Report 2013, 19, IEAGHG, Cheltenham, UK, 2013
[2] Carrasco-Maldonado, F., *et al.*, Oxy-Fuel Combustion Technology for Cement Production – State of the Art Research and Technology Development, *International Journal of Greenhouse Gas Control*, *45*. (2016), Feb., pp. 189-199
[3] Fajardy, M., *et al.*, The Economics of Bioenergy with Carbon Capture and Storage (BECCS) Deployment in a 1.5 °C or 2 °C World, *Global Environmental Change*, *68*. (2021), 102262
[4] Dai, G., *et al.*, Experimental and Kinetic Study of N_2O Thermal Decomposition in Pressurized Oxy-Combustion, *Fuel*, *346* (2023), 128323
[5] Hendriks, C. A., *et al.*, Emission Reduction of Greenhouse Gases from the Cement Industry, *Proceedings*, 4th International Conference on Greenhouse Gas Control Technologies, 1998, Interlaken, Switzerland, pp. 939-944
[6] Buhre, B. J. P., *et al.*, Oxy-Fuel Combustion Technology for Coal-Fired Power Generation, *Progress in Energy and Combustion Science*, *31* (2005), 4, pp. 283-307
[7] Hills, T., *et al.*, Carbon Capture in the Cement Industry: Technologies, Progress, and Retrofitting, *Environmental Science & Technology*, *50* (2016), 1, pp. 368-377
[8] Zeman, F., Oxygen Combustion in Cement Production, *Energy Procedia*, *1* (2009), 1, pp. 187-194
[9] Wall, T., *et al.*, An Overview on Oxy-Fuel Coal Combustion – State of the Art Research and Technology Development, *Chemical Engineering Research and Design*, *87* (2009), 8, pp. 1003-1016
[10] Toftegaard, M. B., *et al.*, Oxy-Fuel Combustion of Solid Fuels, *Progress in Energy and Combustion Science*, *36* (2010), 5, pp. 581-625
[11] Buhre, B. J., *et al.*, Oxy-Fuel Combustion Technology for Coal-Fired Power Generation, *Progress in Energy and Combustion Science*, *31* (2005), 4, pp. 283-307
[12] Chen, L., *et al.*, Oxy-Fuel Combustion of Pulverized Coal: Characterization, Fundamentals, Stabilization and CFD Modeling, *Progress in Energy and Combustion Science*, *38* (2012), 2, pp. 156-214
[13] Stanger, R., *et al.*, Oxy-Fuel Combustion for CO_2 Capture in Power Plants, *International Journal of Greenhouse Gas Control*, *40* (2015), Sept., pp. 55-125
[14] Gimenez, M., *et al.*, The Oxycombustion Option, *International Cement Review*, *37* (2014), Jan., p. 38
[15] Kantee, U., *et al.*, Cement Manufacturing Using Alternative Fuels and the Advantages of Process Modelling, *Fuel Processing Technology*, *85* (2004), 4, pp. 293-301
[16] Scheffknecht, G., *et al.*, Oxy-Fuel Coal Combustion – A Review of the Current State-of-the-Art, *International Journal of Greenhouse Gas Control*, *5* (2011), Suppl., pp. S16-S35
[17] Garcia-Maraver, A., *et al.*, Determination and Comparison of Combustion Kinetics Parameters of Agricultural Biomass from Olive Trees, *Renewable Energy*, *83* (2015), Nov., pp. 897-904
[18] Mladenović, M., *et al.*, Denitrification Techniques for Biomass Combustion, *Renewable and Sustainable Energy Reviews*, *82* (2018), Part 3, pp. 3350-3364

[19] Proskurina, S., *et al.*, Biomass for Industrial Applications: The Role of Torrefaction, *Renewable Energy*, *111* (2017), Oct., pp. 265-274
[20] Song, X., *et al.*, Ultrasonic Pelleting of Torrefied Lignocellulosic Biomass for Bioenergy Production, *Renewable Energy*, *129* (2018), Part A, pp. 56-62
[21] Wang, X., *et al.*, Numerical Study of Biomass Co-Firing under Oxy-MILD Mode, *Renewable Energy*, *146* (2020), Feb., pp. 2566-2576
[22] Wang, M., *et al.*, Numerical Simulation of Oxy-Coal Combustion in a Rotary Cement Kiln, *Applied Thermal Engineering*, *103* (2016), June, pp. 491-500
[23] Yin, C., *et al.*, New Weighted Sum of Gray Gases Model Applicable to Computational Fluid Dynamics (CFD) Modeling of Oxy-Fuel Combustion: Derivation, Validation, and Implementation, *Energy & Fuels*, *24* (2010), 12, pp. 6275-6282
[24] Marin, O., *et al.*, Simulating the Impact of Oxygen Enrichment in a Cement Rotary Kiln Using Advanced Computational Methods, *Combustion Science and Technology*, *164* (2001), 1, pp. 193-207
[25] Peters, A. A. F., Weber, R., Mathematical Modeling of a 2. 25 MWt Swirling Natural Gas Flame. Part 1: Eddy Break-up Concept for Turbulent Combustion; Probability Density Function Approach for Nitric Oxide Formation, *Combustion Science and Technology*, *110-111* (1995), 1, pp. 67-101
[26] Hanson, R. K., Salimian, S., Survey of Rate Constants in the N/H/O System, in: *Combustion Chemistry*, Springer Verlag, Berlin, 2018, Chapter 6, pp. 361-421
[27] De Soete, G. G., Overall Reaction Rates of NO and N_2 Formation from Fuel Nitrogen, *Proocedings*, 15th Symposium (International) on Combustion, Tokio, Japan, pp. 1093-1102, 1975
[28] Jones, J., *et al.*, Modelling NOx Formation in Coal Particle Combustion at High Temperature: an Investigation of the Devolatilisation Kinetic Factors, *Fuel*, *78* (1999), 10, pp. 1171-1179
[29] Ghani, M. U., Wendt, J. O., Early Evolution of Coal Nitrogen in Opposed Flow Combustion Configurations, *Proceedings*, 23rd Symposium (International) on Combustion, Orleans, France, pp. 1281-1288, 1991
[30] Hill, S., Smoot, L. D., Modeling of Nitrogen Oxides Formation and Destruction in Combustion Systems, *Progress in Energy and Combustion Science*, *26* (2000), 4-6, pp. 417-458
[31] Alvarez, L., *et al.*, Biomass Co-Firing under Oxy-Fuel Conditions: A Computational Fluid Dynamics Modelling Study and Experimental Validation, *Fuel Processing Technology*, *120* (2014), Apr., pp. 22-33
[32] Hein, K., Bemtgen, J., EU Clean Coal Technology – Co-Combustion of Coal and Biomass, *Fuel processing technology*, *54* (1998), 1-3, pp. 159-169
[33] Spliethoff, H., Hein, K., Effect of Co-Combustion of Biomass on Emissions in Pulverized Fuel Furnaces, *Fuel Processing Technology*, *54* (1998), 1-3, pp. 189-205
[34] Kiga, T., *et al.*, Characteristics of Pulverized-Coal Combustion in the System of Oxygen/Recycled Flue Gas Combustion, *Energy Conversion and Management*, *38* (1997), Suppl., pp. S129-S134
[35] Molina, A., Shaddix, C. R., Ignition and Devolatilization of Pulverized Bituminous Coal Particles during Oxygen/Carbon Dioxide Coal Combustion, *Proceedings of the Combustion Institute*, *31* (2007), 2, pp. 1905-1912
[36] Andersson, K., *et al.*, Radiation Intensity of Lignite-Fired Oxy-Fuel Flames, *Experimental Thermal and Fluid Science*, *33* (2008), 1, pp. 67-76

Paper submitted: January 19, 2024
Paper revised: May 1, 2024
Paper accepted: June 24, 2024
2024 Published by the Vinča Institute of Nuclear Sciences, Belgrade, Serbia.
This is an open access article distributed under the CC BY-NC-ND 4.0 terms and conditions.